21670TELKOMNIKA Telecommunication, Computing, Electronics and Control
Vol. 19, No. 6, December 2021, pp. 1935~1947
ISSN: 1693-6930, accredited First Grade by Kemenristekdikti, Decree No: 21/E/KPT/2018
DOI: 10.12928/TELKOMNIKA.v19i6.21670

Quality control in GNSS reflectometry method for tide observations

Agung Syetiawan[1], Dudy Darmawan Wijaya[2], Irwan Meilano[3]
[1]Research division, Geospatial Information Agency, Bogor, Indonesia
[2,3]Geodesy and Geomatics Engineering, Faculty of Earth Sciences, Institut Teknologi Bandung, Bandung, Indonesia

Article Info

Article history:

Received Mar 13, 2021
Revised Oct 8, 2021
Accepted Oct 19, 2021

Keywords:

Control quality
GNSS-R
Periodogram
Tide

ABSTRACT

Recently, the reflected signals from global navigation satellite systems (GNSS) have been utilized to observe coastal tides, and it has been found that this method provides promising results. Although this method is promising, there remain problems related to accuracy of the observed tides. The purpose of this study was to improve the accuracy by employing an optimal spectral method in the quality control scheme. The quality control process is carried out by setting parameters to achieve the best possible frequency correlated with sea levels such as estimation of the noise frequency range, frequency amplitude power selection, and selection of peak frequency to noise ratio. The results using the data at Morotai station showed that the amplitude power less than 5 comes from low-frequency signals and hence it is an indicator that the Lomb-Scargle periodogram (LSP) fails to determine the dominant frequency. In addition, the result of the peak frequency to noise ratio shows a value of 2.7, meaning that the peak frequency of the LSP signal is at least 2.7 times greater than the signal noise. Quality control sensitivity settings are very effective in determining the reflectors height coming from the sea level. The periodogram visualization can be used to decide which LSP is significant.

Corresponding Author:

Agung Syetiawan
Research division, Geospatial Information Agency
Jakarta-Bogor Street Km. 46, Cibinong 16911, Jawa Barat, Indonesia
Email: agung.syetiawan@big.go.id

1. INTRODUCTION

The height measurement on the Earth's surface must be referenced to the zero points, also known as the datum plane. In its application, the vertical datum is realized in the form of pillars. Furthermore, defining the vertical datum in Indonesia is carried out by determining the orthometric height of a pillar as a datum point which is called the vertical control network/*Jaring Kontrol Vertikal* (JKV). Ideally, the orthometric height is determined with respect to the equipotential surface of the Earth which is often referred to as the geoid [1], [2]. However, the current Indonesian geoid model still has non-uniform accuracy. Therefore, the geoid fields were approached using mean sea level values. For this reason, the determination of the orthometric height requires observation of the tide for at least 18.6 years [3], [4]. Tide observation is needed to get the pillar height value refers to the mean sea level in ideal conditions.

Nowadays, tide observation can be carried out using in situ and satellite-based methods. In situ methods, such as a tide gauge, measure local sea level heights relative to a fixed reference point. The reference point is usually realized by a geodetic pillar that is installed on the ground surface. Disadvantages

of the tide gauge method are: it only provides tide time-series information at one point and the reference pillar is highly affected by the effects of land deformation, sediment transfer, and subsidence around the tidal station [5].

Another commonly used method is satellite altimetry, which can provide information related to global sea surface height (SSH) with high spatial and temporal resolution [6]. Satellite altimetry measures the distance between the satellite and sea surface using radar technology and the resulted height refers to the global terrestrial reference frame [7]. SSH from altimetry observations is not affected by land surface changes. Unfortunately, SSH accuracies in coastal areas and shallow waters seem to be inaccurate, this is due to the disturbance of the reflected altimetric waveform in coastal areas [8], [9]. As an archipelago, Indonesia has many shallow water covered areas. This characteristic needs to be thoroughly considered when using altimeter satellites as data sources in coastal areas.

The use of tide gauge and altimetry satellite technology in coastal areas is indeed still not optimal due to inadequate spatial and temporal resolution for observing complex sea levels [10]. Currently, another alternative method is being developed to observe the sea level by utilizing the global navigation satellite systems (GNSS) multipath signal [5], [11]. This method is known as GNSS-reflectometry or commonly abbreviated as GNSS-R. The number of GNSS satellites is now increasing and available all day, so that it can produce observations of sea level in coastal areas with higher temporal resolution. These advantages provide unique opportunities to further develop GNSS-R method in many aspects.

The GNSS-R method utilizes multipath signals that have long been considered as noise in geodetic precise positioning applications. When the GNSS signal hits the surface of the reflection plane, the multipath signal carries information related to the physical characteristics of the reflection plane such as a surface [12]. Reflections of satellite signals from the surface around the receiving antenna mix with the direct signals resulting in multipath errors in measurement code, carrier phase, and signal-to-noise ratio [13]. The frequency and amplitude of the multipath signals have a strong correlation with the characteristics of the environment around the observer. Therefore, multipath signals can be used to study the phenomena and characteristics of the reflection plane such as soil moisture measurement [14], snow depth [15], [16], tidal observations [17], [18], and water content in plants [19].

Results from Larson *et al.* in the Kachemak Bay region of Alaska show that a geodetic-type global positioning system (GPS) receiver installed near the coast can accurately measure sea level [20]. In addition, sea level observations generated from GNSS-R at the Onsala Space Observatory produce high correlation values when compared to sea level observations from tide gauge sensors [5]. Another study conducted by Chen *et al.* [21] used GPS satellites with low temporal resolution tide results, an RMSE value of 0.34 m and a correlation of 87%. A similar study was conducted by Lee *et al.* [22] using Taiwan coastal observation and assessment station (TaiCOAST), yields an root mean square error (RMSE) value above 1 m and a correlation of 13%. There are problems related to the accuracy and correlation of the tide observations generated from the GNSS-R.

The accuracy of GNSS-R results is strongly dependent on the quality control applied. Several approaches in signal-to-noise ratio (SNR) data processing include the application of elevation angle correction [23] and dynamic correction of the reflection plane [20]. Dynamic correction eliminates errors due to dynamic changes of the reflection plane. Larson *et al.* [17] found that the Fresnel zone starts to include the shore at a satellite elevation angle of more than 13º. Larson *et al.* [20] used a quality control technique by normalizing the spectrogram peak at 1 dB-Hz and making the peak-to-noise ratio criteria greater than 3 in the periodogram analysis.

Quality control plays an important role in SNR data processing. According to Song *et al.* [24] to improve the accuracy and effectiveness of processing results, several ways can be done, including denoising raw data, controlling parameters during data processing, or filtering/denoising after data processing. Implementing quality control and adding satellite segments can improve accuracy and temporal resolution. Therefore, it is necessary to develop an efficient and flexible quality control method for periodogram analysis. The purpose of this research was to improve the accuracy by employing an optimal spectral method in the quality control scheme.

2. RESEARCH METHOD

Sea level observation research using the GNSS-R method was conducted at the Morotai station. Such a station was chosen because of the availability of complete GNSS and tidal data. Morotai tidal station is located at the port of Morotai, Pulau Morotai Regency, North Maluku Province at latitude 2° 0' 59" north and longitude 128° 16' 49" east (can be seen in Figure 1). The Morotai station is one of the tidal stations belonging to the Geospatial Information Agency which is designed to monitor sea level and is part of the tsunami early warning system in Indonesia.

Figure 1. Location of Morotai tide station

The research stages can be seen in the research flow chart in Figure 2. The research is divided into 2 stages, namely the data preparation and data processing. The data preparation includes translating GNSS data by extracting SNR data from the receiver independent exchange (RINEX) file. After that, determine the azimuth and elevation angle of the satellite which is calculated from the receiver coordinate information obtained in the RINEX header and the satellite position coordinates using precise orbit information (*.sp3). Receiver coordinate information uses a Cartesian coordinate system with receiver position accuracy not more than 50 m [25]. The satellite observations (in GPS time, seconds of day) are then extracted together with the SNR observations at the L1 and L2 frequencies. Furthermore, at the data processing stage, mapping the reflection zone or first Fresnel zone (FFZ) is first carried out to see if the reflection of the GNSS signal coming from the sea. Azimuth angles of the reflected signals are later used to calculate the reflector height. The next step is to separate the multipath signals from the direct ones (detrending the composite signals). Before detrended SNR process, the SNR data is changed from the decibel scale unit to a linear scale such as volts. After separating the multipath signals, the reflected signal from the sea is then analyzed using the Lomb-Scargle periodogram (LSP) method to determine the reflector height above sea level [18]. Finally, the quality control process is carried out to get the dominant frequency bands and hence to get the best quality of tide observations.

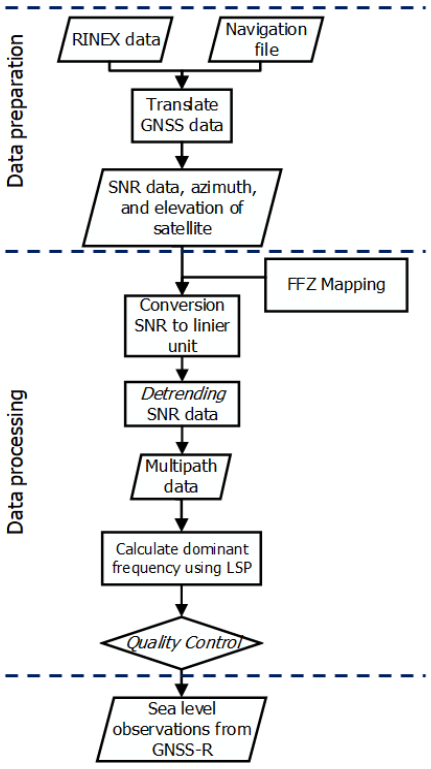

Figure 2. GNSS-R research flowchart

2.1. Signal to noise ratio (SNR) analysis

GNSS observations are inseparable from noises that affect the travel of electromagnetic waves from satellites to antenna receivers on Earth. In geodetic positioning, these noises must be eliminated to improve positional accuracy. Oppositely, GNSS remote sensing exploits such noises to obtain other interesting information. In simple terms, the multipath effect on the surface of the reflection plane can be found in the SNR observations. SNR is the ratio between signal and noise power, whose value is used to indicate the quality of the GNSS signals. By eliminating the contribution of signal errors, SNR data for single observations of satellites and receivers can be modeled as (1) [26].

$$SNR(e) = A(e) \sin\left(\frac{4\,\pi\,H_R}{\lambda} \sin e + \theta\right) \quad (1)$$

Where e is the elevation angle of the GNSS satellite referring to the horizon, λ is the GNSS wavelength, θ is the phase difference, H_R is the vertical distance between the antenna phase center (APC) to the surface of the horizontal reflection, and A(e) represents the amplitude of the SNR data.

The SNR representation is time-dependent because the value of e is a function of time. The signal received by the receiver is a composite of a direct signal and a reflected signal passing through a surface plane, as can be seen in Figure 3. The value of ε is the elevation angle of the satellite. The SNR analysis technique uses direct signals and reflected signals to analyze SNR patterns based on the coherent conditions of the two signals [27]. To get the multipath signal, direct signal can be eliminated using low order polynomial fitting. The detrended SNR process is accomplished by separating the composite signal from the fit value of the polynomial results so that the SNR value will be obtained which only contains the reflected signal. In GNSS-R, the elimination of direct trends using a low-order polynomial aims to produce a height reflector value (H_R). In this study, a 3rd degree polynomial was used during the detrended process. After removing the direct trend, we will finally get a multipath pattern which is described as (2) [26].

$$dSNR = A\,cos(4\pi H\lambda^{-1}\,sin\,\theta + \phi) \quad (2)$$

Where dSNR is the detrended SNR representing the effect of the reflected signal on the SNR data, A is the amplitude, H is the reflector height, and ϕ is the phase.

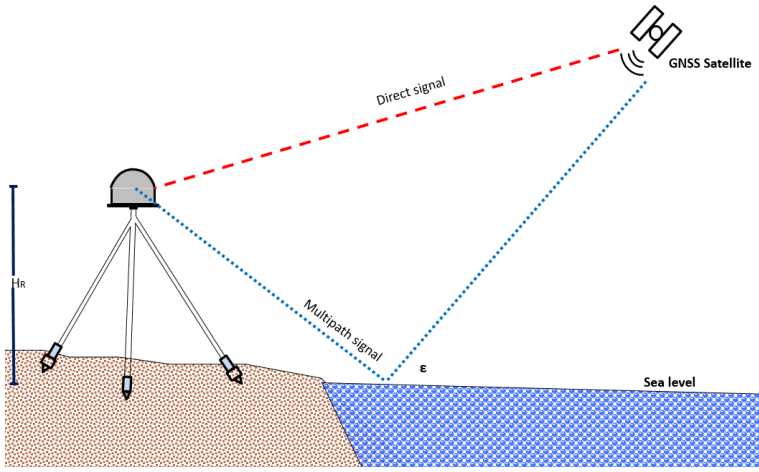

Figure 3. GNSS-reflectometry geometry

Furthermore, the multipath signal is then analyzed using the LSP method, which calculates the vertical distance of the reflection plane surface based on the dominant frequency of the multipath signal from the peak value of the wave [5]. The LSP is an algorithm for detecting and categorizing periodicity in an uneven sample series data [28], [29]. The LSP allows for efficient calculations resulting in periods of oscillation. The LSP estimates the Fourier power as a function of the oscillation period. The reflection plane characteristics of the GNSS signal are recorded as an oscillation in the SNR series. The LSP algorithm such as the fast fourier transform (FFT) is used to estimate the temporal change in the interferogram dominant frequency of SNR data.

2.2. Quality control parameters in GNSS-R data processing

Statistically, the estimated peak from one LSP shall not be considered as the accurate value. The highest peak value is merely related to the high frequency of the best reflector. In fact, in a set of SNR series, multiple peaks affect the extraction accuracy of the reflector height [24], [30]. This quality control process is used to improve the approximate high quality of the reflector. Furthermore, the quality control process is carried out by setting parameters to select the best frequency. Quality control is used to assess which SNR observations are correlated with sea level. In this study, the quality control parameters used include estimated noise frequency range, selection of minimum frequency amplitude power, and selection of peak frequency to noise ratio.

2.2.1. Frequency noise range

This parameter is a selection of the frequency noise range used in GNSS-R data quality control. Later, from this range, the average frequency noise is calculated from a set of SNR data series. In this study, the effect of non-physical reflectors height was eliminated by removing frequencies whose values are less than 3 and are more than 10. Different frequency ranges can be used to separate the signal and eliminate the non-physical reflector height (R_H), where R_H is less than 3 the result of the reflected signal from the coast (low frequency), while R_H more than 10 is high frequency noise [31].

2.2.2. Amplitude frequency power

A setting on the amplitude of the frequency is used to determine the power of the minimum frequency. The amplitude power of a single signal peak is highly correlated with the surface of the reflection plane [25]. Meanwhile, the signal frequency which has small amplitude is the noise frequency and, in this application, it should be discarded.

2.2.3. Peak frequency to noise ratio

This parameter is the value used to see the comparison between the strength of the dominant frequency compared to the average frequency noise. A good reflected signal is when the power of the dominant frequency has a single peak. This means that there is no noise from other frequencies in the processed multipath set of observations.

2.3. Characteristics of the Morotai station (CMOR)

The equipment used for recording tidal data is radar sensor, pressure gauge, and float gauge. The original data records are sampled every minute, but this study uses hourly data. Apart from recording tide data, the Morotai station is also equipped with a GNSS receiver that is installed at the top of the tidal equipment house at the Morotai port (see its illustration in Figure 4). The GNSS receiver designed by Trimble Alloy with choke rings antenna model TRM59800 is employed. In addition, the GNSS antenna is also equipped with a SCIS radome type. The receiver can record signals from the GPS, global navigation satellite system (GLONASS), Galileo, and satellite-based augmentation system (SBAS). The GNSS receiver will then be used as an alternative tool for observing the sea level around Morotai port using the GNSS-R technique.

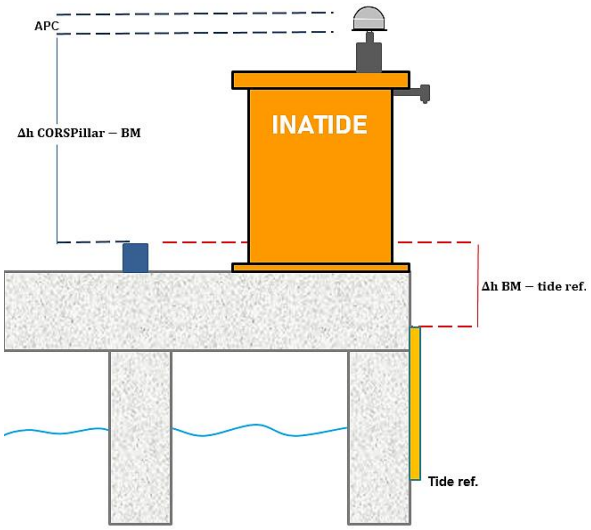

Figure 4. GNSS antenna geometry to sea level reference

The primary result from the GNSS-R observation is the vertical distance between the APC and the water surface so that there is a different reference with tide observation from tide gauge sensor. The tide gauge sensor refers to zero palm reference. Therefore, to get the tide observations referring to the same reference (zero palm reference), the tide observation from the GNSS-R needs to be corrected. An illustration of the condition of the tidal station and GNSS antenna at the port of Morotai can be seen in Figure 4. Due to the limited vertical height information from the APC to the zero-palm reference, the vertical height measurement is carried out using GNSS-leveling. Furthermore, the height difference from bench mark (BM) to zero palm reference uses leveling observation data. The tidal range at Morotai station shows a value of 2.2 m, with the type of tide being a mixed tide prevailing semidiurnal. Therefore, determining sea level using GNSS-R is a challenge in this area.

3. RESULTS AND ANALYSIS

3.1. Selection of satellite azimuth and elevation angle

The first Fresnel zone is the level of interference based on the characteristics of the reflection plane and its distance to the antenna. Fresnel zone changes are closely related to the satellite elevation angle, Fresnel zone becomes smaller when the elevation angle of the satellite increases or approaches the GNSS antenna. Figure 5 shows an illustration related to the Fresnel zone at the CMOR station, Morotai. The size of the Fresnel zone ellipse is closely related to the height of the reflector, the satellite elevation angle, and the signal frequency used [25]. Therefore, this Fresnel zone mapping is used to make it easier to determine the correct azimuth angle and satellite elevation at the research location. The illustration of the Fresnel zone is depicted in Figure 5, assuming the height between the reflection plane and the GNSS antenna is 6 meters. Satellite elevation angles are drawn in various colors, in red (5°), light blue (10°), yellow (15°), green (20°), and dark blue (25°). The GNSS-R application uses the reflected multipath signal from the sea to calculate the reflector height. Based on the Fresnel zone mapping, the azimuth angles used in this study are within the ranges 0-20º and 200-360º, within which the signals contain multipath effects originating from the sea.

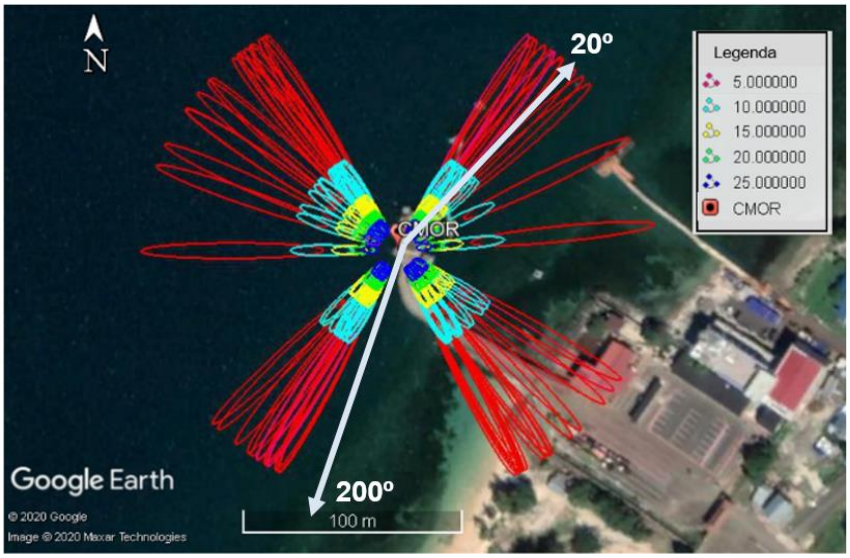

Figure 5. The first Fresnel zone at the CMOR station plotted by assuming the fixed reflector height is 6 meters

In Figure 6, the SNR data of the L1 frequency shows a variation from ~ 30 dB to ~ 50 dB. By using a low pass filter, the SNR data seems to oscillate especially for the satellites whose elevations are less than 30°, as is indicated by red line in Figure 6. This SNR oscillation is a result of the multipath effect. Furthermore, as can also be seen in Figure 6, the oscillations hardly occur at elevations above 25º, this may indicate that above 25º elevation angle multipath signals diminish. In addition, for the elevation above 25º, the reflected signal may come from the harbor building or coast, as can be seen in Figure 5. According to Song *et al.* [24], determining the satellite elevation limit at 5º elevation is used to eliminate problems due to atmospheric bias at very low satellite elevation angles. Therefore, based on the results of the analysis in this section, the satellite elevation angles used to calculate the reflector height are in the range of 5-25º.

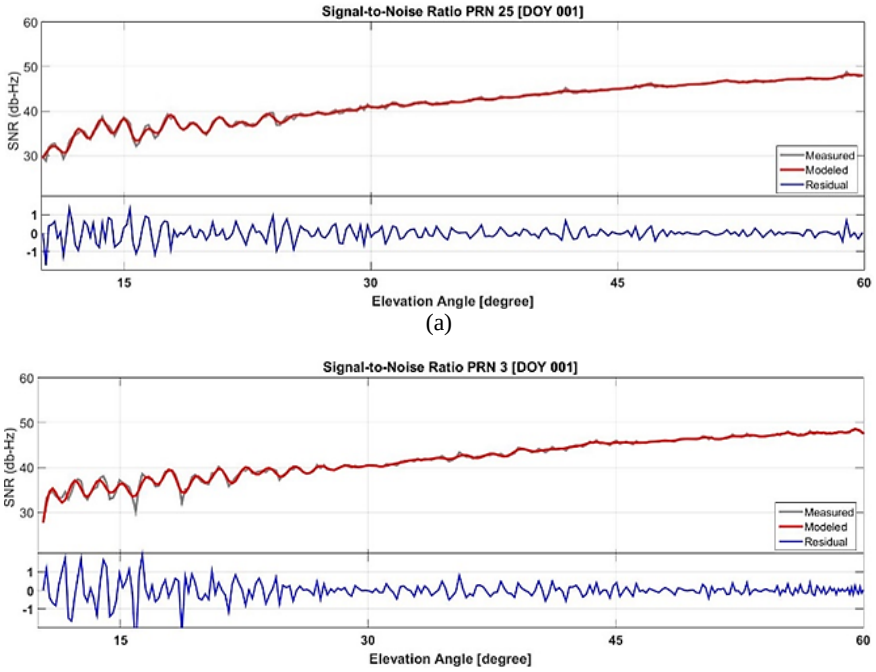

Figure 6. The SNR oscillations at the CMOR station for day of year (DOY) 001: satellite pseudo random number (PRN) (a) 25 and (b) 3

3.2. Detrended multipath data

The results of the PRN 5 satellite multipath signal detrending process at DOY 032 can be seen in Figure 7, the green dot is the SNR observation data in the form of a composite signal. Meanwhile, the red line is a trend of low orders polynomial fitting consisting of a direct signal. Direct signals appear to increase slowly as the elevation angle increases. On the other hand, the multipath signal (blue line) is generated by subtracting polynomial fit from the raw SNR observation data, so that the direct signal effect has been removed from the SNR data. Without the multipath effect, the SNR observations increase slowly as the elevation angle of the satellite increases [32]. The direct component of the signal looks like a periodic pattern, while the reflected signal (multipath) looks like an oscillating part. The effect of the reflected signal is much more dominant than the direct signal.

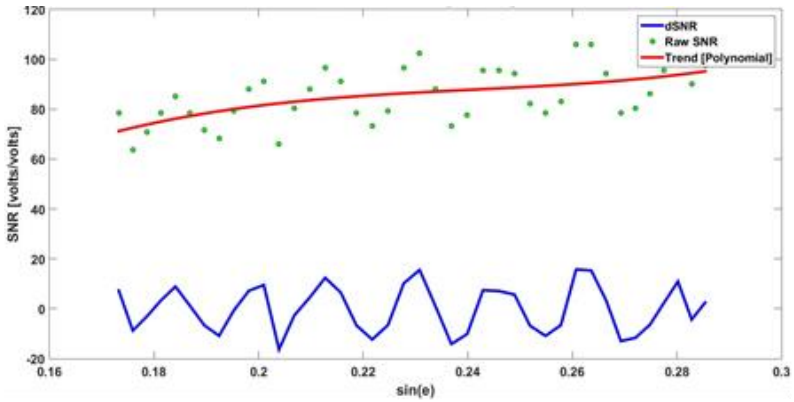

Figure 7. Process of detrending the multipath signal

3.3. Lomb-Scargle periodogram results

3.3.1. Power amplitude frequency

The LSP calculates the normalized periodogram from sequential SNR, along the satellite arc over the specified satellite elevation range. The success of estimating the reflector height can be seen in the LSP

results, where only a single peak value for a specific frequency. Furthermore, such a frequency is called the dominant frequency of the multipath signal, as can be seen in Figure 8. In Figure 8, the maximum amplitude of satellite 5 shows a value at a frequency of ~ 6 m, meaning that this value represents the height of the reflector deducing from the SNR reflection from satellite 5. The peak value of the periodogram is expressed in terms of the amplitude of the frequency. In addition, amplitude power is used to inspect the significance of the multipath signal. The amplitude powers of the frequencies of satellites PRN 1, 4, 6, and 16 are shown in Figure 9. A double peak is seen on satellite 1, while frequencies with a similar peak are seen on satellite 16. The double peaks are caused by the presence of other dominant frequencies, so there is uncertainty about the estimation results of the reflector height. Meanwhile, a similar peak frequency comes from the noise frequency around the antenna. Another phenomenon is also seen in satellites 4 and 6 which produce a reflector height estimate of 10. The peak frequency value is 10 because the estimated periodogram peak is at the maximum frequency limit set during LSP processing. This phenomenon occurs due to the inability of the LSP to determine the significant frequency of a series of problematic SNR observations.

Besides the problem of noise at low frequencies, which is due to the influence of the location around the antenna, other problems may occur namely the frequencies whose amplitude power is very small, as can be seen in Figure 10. It occurs due to the effect of rising and setting of the satellite, which also affects the others SNR satellites. There is no significant frequency found, yielding the estimated amplitude of the frequency is very small when calculated in the spectral domain, as can be seen in Figure 11. The satellite rise is seen at an elevation of 11.9º to an elevation of 12.15º, while a satellite set is seen at an elevation of 12.15º to an elevation of 11.75º. This phenomenon causes the estimated value of the reflector height to be 10 because the estimated peak of the periodogram reaches the specified maximum frequency limit.

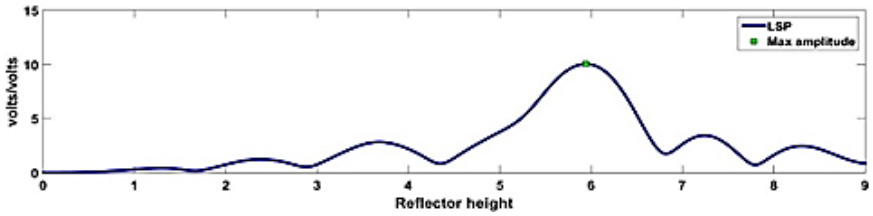

Figure 8. Dominant frequency in the spectral domain

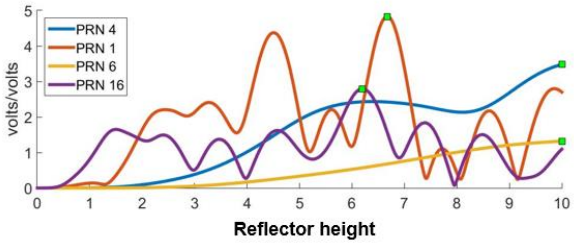

Figure 9. Amplitude power of the frequency in the spectral domain

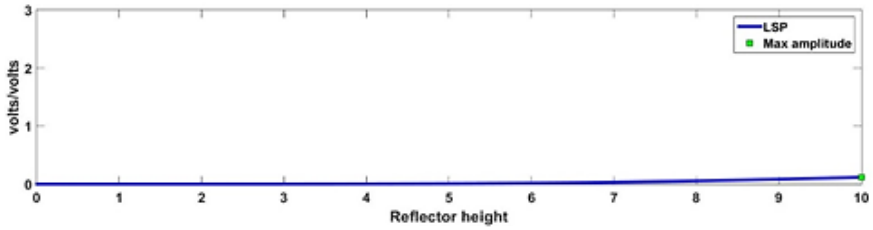

Figure 10. The periodogram of a series of SNR observations on satellite rise and set

From this LSP analysis it can be seen that the amplitude power of the frequency less than 5 is affected by noise, thus making the estimation of the reflector height inaccurate. These noisy frequencies represent the characteristics of the reflection plane, originating from the coast and/or land reflections. In

addition, the amplitude power of the frequencies less than 5 is caused by the failure of the LSP to calculate the dominant frequency from a series of SNR observations. The failure can occur during the detrending process of multipath signal separation, the effect of direct signals is still carried over to multipath observations. Another failure is due to the satellite tracking on the elevation of the satellite rise and set which influences the determination of the dominant frequency during LSP processing. Therefore, the amplitude power can be used as quality control to determine which frequency corresponds to the plane of reflection.

3.3.2. Ratio of peak frequency to noise

The amplitude power of the frequency is closely related to the characteristics of the reflection plane. Unfortunately, amplitude power cannot be directly used to determine reflector height accurately. Figure 12 shows the power of the frequency at the observed reflector height. The x-axis shows the height of the reflector, while the y-axis is the time and the color range shows the power of the frequency. As can be seen in Figure 12, there is still noise and is considered to be the height of the reflector. The tidal pattern is seen to oscillate over a frequency range of ~ 5 m to ~ 8 m. Figure 12 also shows that the height of the reflector with a value of 10 has an amplitude power of frequency above 5, seen on the light blue scale bar. This means that to get a certain quality of reflector height, it is not enough just to see the amplitude of the frequency. Therefore, another quality control is needed, namely using the ratio of peak frequency to noise. The ratio of peak frequency to noise is used to detect multiple peaks in a series of SNR observations. The double peaks give an inaccurate estimation of the reflector height, so they should be discarded.

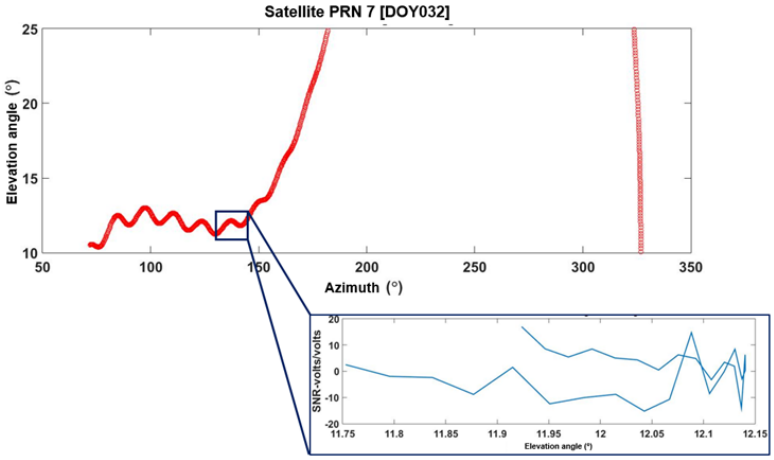

Figure 11. Effects of satellite rise and set on a series of SNR observations

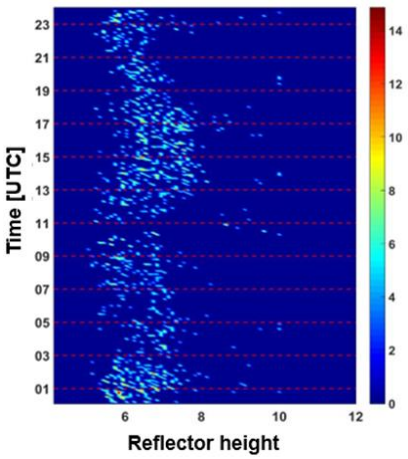

Figure 12. Scalogram power frequency from reflector height

Figure 13 shows the results of the multipath signal periodogram on the satellite PRN 05 and 31 for DOY 032. To calculate the peak-to-noise ratio, the first thing is to determine the noise frequency range related to the physical characteristics of the reflection plane in a multipath signal. The range of physical frequency noise is determined at a frequency value of 3 to 10, discarding a frequency value outside that range, as can be seen in the dotted black line in Figure 13. Thus, the noise frequency outside this range does not correlate with the characteristics of the reflection plane. After that, the calculation of the peak frequency to noise ratio is done by dividing the maximum amplitude (peak frequency) by the average amplitude of the noise range. The maximum amplitude is represented by a green square. Meanwhile, the average amplitude is represented by a dashed line in red and the ratio of the peak frequency to noise (noise peak criteria) is represented by a dashed line in light blue.

As seen in Figure 13(a), satellite 5 has a dominant frequency amplitude greater than 5 volts/volts, with an estimated reflector height of ~ 7m. However, when viewed in detail, there are several frequencies with similar amplitudes power, namely at frequencies of ~ 4.8 m and ~ 2.5 m. As seen on satellite 31 in Figure 13(b), there is a peak amplitude frequency with an estimated reflector height of ~ 6 m. The double peak on the LSP analysis creates uncertainty for the resulting reflector height value. Therefore, quality control cannot only look at the amplitude of the peak frequency.

The peak frequency to noise ratio takes into account frequencies with similar amplitudes power over a specific frequency range. The quality control will avoid errors in the estimation of reflector height. If the more noise frequency with large amplitude power, the average amplitude value will increase. This means that

noise is more dominant than multipath signals originating from the reflection plane. In contrast to the single dominant frequency shown in Figure 8. The noise frequency has a small amplitude, while the frequency related to the reflection plane is shown as the peak of the periodogram.

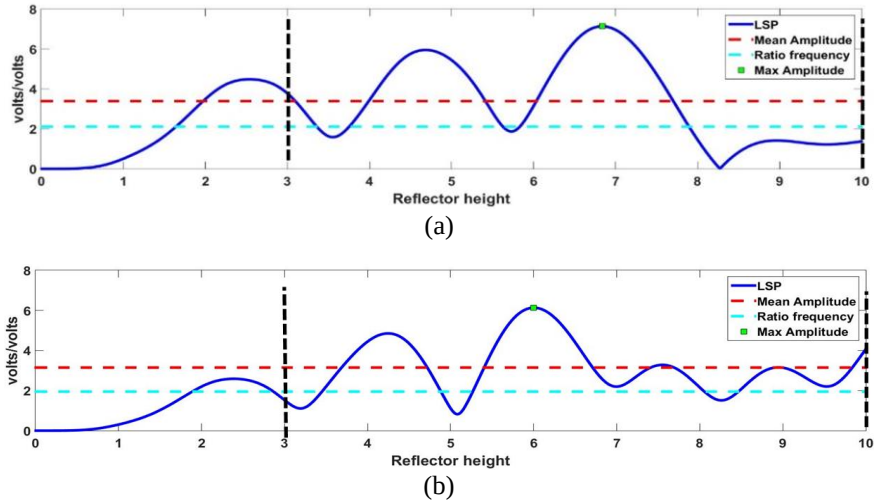

Figure 13. SNR periodogram on: (a) satellite PRN 5 and (b) satellite PRN 31

Based on the visualization of the periodogram, the ratio used is a minimum value of 2.7 to get the best reflector height. The ratio value less than 2.7 shows the noise frequencies contained in a series of SNR observations. This ratio means that the peak frequency of the LSP (dominant frequency) is at least 2.7 times greater than the signal noise. Therefore, a ratio value of less than 2.7 is discarded in determining the reflector height, even though the amplitude power is strong. The more noise in the SNR data set, so the higher of average amplitude and the unrealistic reflector height value. This quality control process is very important, to remove signals that do not come from reflection from the water.

The use of frequency ratio in the quality control process needs to be considered. Since the ratio criteria can see noise frequencies in a series of SNR data, there are problems with frequencies that have very small amplitude powers. As can be seen in Figure 14, the power of the periodogram amplitude on the satellite PRN 29 is ~ 0. If the ratio of the dominant frequency to noise is calculated, the results of the ratio criteria are ~ 3.5. This ratio criterion value is very unrealistic because the estimation of the reflector height is generated from the peak of the periodogram with very small amplitude power. Therefore, for these two quality controls, both the determination of minimum amplitude and the ratio of periodogram peak to noise must be used simultaneously to obtain a reliable estimate of reflector height.

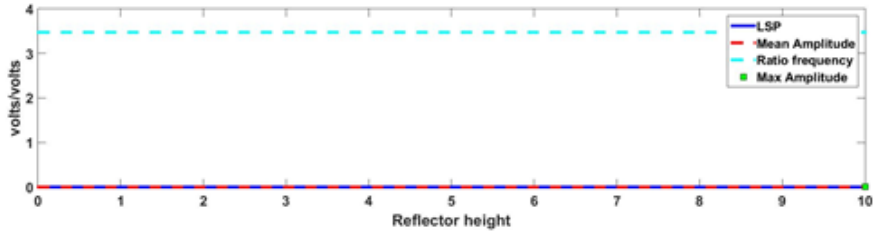

Figure 14. SNR periodogram on the satellite PRN 29

3.4. The results of the GNSS-R data analysis

The quality controls used to obtain the best estimation of reflector height are presented in Table 1. Quality control is used to ensure that the reflector height estimate does not result from signal noise. The application of quality control makes the reflector height estimation results even better, as can be seen in Figure 15. Before quality control was applied, the resulting reflector height contained a lot of noise, as can be seen in Figure 15(a). Therefore, quality control makes the tide observations from the GNSS-R close to the same as those from tide gauge sensor, as can be seen in Figure 15(b). The sensitivity of quality control is

highly meaningful on the final results of tidal observations using GNSS-R. Thus, quality control in GNSS-R data processing is very effective in obtaining sea level observations with strong confidence. The determination of the reflector height is calculated from APC to sea level so that quality control is very dependent on the APC geometry to sea level. Therefore, the application of quality control must adjust the geometry of the reflector height in the region.

Table 1. The quality control used in this research

Quality control	Parameter	Information
Noise frequency range	3-10	The effect of non-physical peak reflector height is eliminated by removing a noise value of less than 3 and an RH value of more than 11 [20].
Amplitude power	>5 V/V	LSP visualization results
Ratio of peak frequency to noise	>2,7	LSP visualization results
Selection of satellite azimuth	0-20º and 200-360º	Fresnel zone mapping result
Selection of satellite elevation angle	5-25º	Fresnel zone mapping and lowpass filtering result

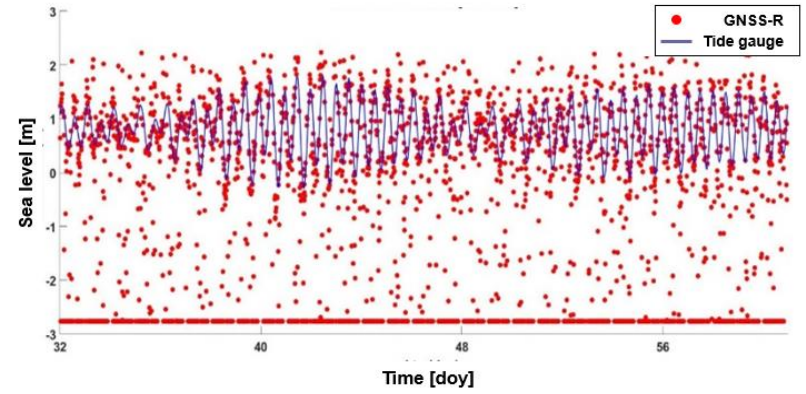

(a)

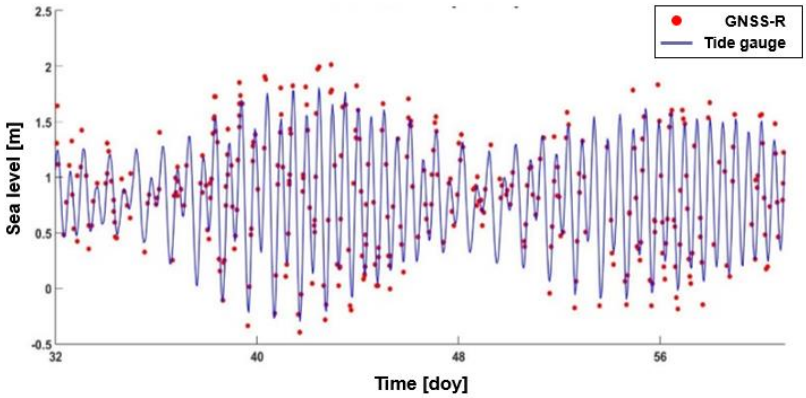

(b)

Figure 15. The results of the GNSS-R tide observation: (a) before quality control and (b) after quality control

4. CONCLUSION

The success of the reflector height estimation can be seen in the LSP results, where only one single frequency has a peak periodogram. The peak value of the periodogram is expressed in terms of the amplitude of the frequency. In addition, amplitude power is used to see the significance of the multipath signal frequency. The power of the amplitude of the frequency is highly correlated with the characteristics of the reflection plane. In the LSP processing, rising and setting the satellite trajectory gives a significant influence in determining the dominant frequency. The effect of satellite rise and set in an SNR data series can be seen from the results of the amplitude power of the frequency. Therefore, the separation of the ascending and descending satellite trajectories is very important to obtain an estimate of the high quality reflector. The quality control of the ratio of the peak frequency compared to noise is used to see the dominance of the peak frequency of the LSP signal (dominant frequency) to the surrounding noise signal. The periodogram

visualization can be used to decide which LSP is significant. The sensitivity of quality control is highly meaningful on the final results of tidal observations using GNSS-R. Thus, quality control in GNSS-R data processing is very effective in obtaining sea level observations with strong confidence.

ACKNOWLEDGEMENTS

This research is supported by the Ministry of Research and Technology/National Research and Innovation Agency of the Republic of Indonesia (BP-PTNBH KEMENRISTEK/BRIN 2020 Research Program) under contract number: 2/E1/KP.PTNBH/2020. In addition, the authors would also like to thank the Geospatial Information Agency for providing both GNSS and tidal observations data.

REFERENCES

[1] L. S. Heliani, "Evaluation of global geopotential model and its application on local geoid modelling of Java Island, Indonesia," *AIP Conf. Proc.*, vol. 1755, no. 1, Jul. 2016, p. 100005, doi: 10.1063/1.4958534.
[2] C. Gerstenecker, G. Läufer, B. Snitil, and A. Sunantyo, "Determination of a Unified Height Reference System for the Computation of a Local Geoid around the Volcanoes Merapi and Merbabu, Java, Indonesia," in *International Association of Geodesy Symposia*, H. Drewes, A. H. Dodson, L. P. S. Fortes, L. Sánchez, and P. Sandoval, Eds. Berlin: Springer Berlin Heidelberg, vol. 124, 2002, pp. 339–344, doi: 10.1007/978-3-662-04683-8_63.
[3] G. Fotopoulos, "An Analysis on the Optimal Combination of Geoid, Orthometric and Ellipsoidal Height Data," University of Calgary, 2003, doi:10.11575/PRISM/10883.
[4] A. G. P. Shaw and M. N. Tsimplis, "The 18.6yr nodal modulation in the tides of Southern European coasts," *Cont. Shelf Res.*, vol. 30, no. 2, pp. 138–151, 2010, doi: 10.1016/j.csr.2009.10.006.
[5] J. S. Löfgren and R. Haas, "Sea level measurements using multi-frequency GPS and GLONASS observations," *EURASIP J. Adv. Signal Process.*, no. 50, 2014, doi: 10.1186/1687-6180-2014-50.
[6] C. K. Shum, J. C. Ries, and B. D. Tapley, "The accuracy and applications of satellite altimetry," *Geophys. J. Int.*, vol. 121, no. 2, pp. 321–336, 1995, doi: 10.1111/j.1365-246X.1995.tb05714.x.
[7] A. Cazenave and G. Le Cozannet, "Sea level rise and its coastal impacts," *Earth's Futur.*, vol. 2, no. 2, pp. 15–34, Feb. 2014, doi: 10.1002/2013EF000188.
[8] C. K. Shum, N. Yu, and C. S. Morris, "Recent advances in ocean tidal science," *J. Geod. Soc. Japan*, vol. 47, no. 1, pp. 528–537, 2001, doi: 10.11366/sokuchi1954.47.528.
[9] S. Vignudelli *et al.*, "Satellite Altimetry Measurements of Sea Level in the Coastal Zone," *Surv. Geophys.*, vol. 40, no. 6, pp. 1319–1349, 2019, doi: 10.1007/s10712-019-09569-1.
[10] J. Bouffard *et al.*, "Introduction and Assessment of Improved Coastal Altimetry Strategies: Case Study over the Northwestern Mediterranean Sea," in *Coastal Altimetry*, S. Vignudelli, A. Kostianoy, P. Cipollini, and J. Benveniste, Eds. Berlin: Springer Berlin Heidelberg, 2011, pp. 297–330, doi: 10.1007/978-3-642-12796-0_12.
[11] J. Strandberg, T. Hobiger, and R. Haas, "Improving GNSS-R sea level determination through inverse modeling of SNR data," *Radio Sci.*, vol. 51, pp. 1286–1296, 2016.
[12] X. Wang, Q. Zhang, and S. Zhang, "Water levels measured with SNR using wavelet decomposition and Lomb– Scargle periodogram," *GPS Solut.*, vol. 22, 2018, doi: 10.1007/s10291-017-0684-8.
[13] P. Axelrad, K. Larson, and B. Jones, "Use of the Correct Satellite Repeat Period to Characterize and Reduce," Site-Specific Multipath Errors," in *ION GNSS 18th International Technical Meeting of the Satellite Division*, 2005, pp. 2638–2648.
[14] K. M. Larson, E. E. Small, E. Gutmann, A. Bilich, P. Axelrad, and J. Braun, "Using GPS multipath to measure soil moisture fluctuations: Initial results," *GPS Solut.*, vol. 12, no. 3, pp. 173–177, 2008, doi: 10.1007/s10291-007-0076-6.
[15] K. M. Larson, E. D. Gutmann, V. U. Zavorotny, J. J. Braun, M. W. Williams, and F. G. Nievinski, "Can we measure snow depth with GPS receivers ?," *Geophys. Res. Lett.*, vol. 36, pp. 1–5, 2009, doi: 10.1007/s10291-007-0076-6.
[16] F. G. Nievinski and K. M. Larson, "Inverse Modeling of GPS Multipath for Snow Depth Estimation—Part I: Formulation and Simulations," in *IEEE Transactions on Geoscience and Remote Sensing*, vol. 52, no. 10, pp. 6555-6563, Oct. 2014, doi: 10.1109/TGRS.2013.2297681.
[17] K. M. Larson, R. D. Ray, and S. D. P. Williams, "A 10-Year Comparison of Water Levels Measured with a Geodetic GPS Receiver versus a Conventional Tide Gauge," *J. Atmos. Ocean. Technol.*, vol. 34, no. 2, pp. 295–307, Feb. 2017, doi: 10.1175/JTECH-D-16-0101.1.
[18] N. Roussel *et al.*, "Sea level monitoring and sea state estimate using a single geodetic receiver," *Remote Sens. Environ.*, vol. 171, pp. 261–277, 2015, doi: 10.1016/j.rse.2015.10.011.
[19] W. Wan, K. M. Larson, E. E. Small, C. C. Chew, and J. J. Braun, "Using geodetic GPS receivers to measure vegetation water content," *GPS Solut.*, vol. 19, pp. 237–248, 2015, doi: 10.1007/s10291-014-0383-7.
[20] K. M. Larson, R. D. Ray, F. G. Nievinski, and J. T. Freymueller, "The Accidental Tide Gauge: A GPS Reflection Case Study From Kachemak Bay, Alaska," in *IEEE Geoscience and Remote Sensing Letters*, vol. 10, no. 5, pp. 1200-1204, Sept. 2013, doi: 10.1109/LGRS.2012.2236075.
[21] F. Chen, L. Liu, and F. Guo, "Sea Surface Height Estimation with Multi-GNSS and Wavelet De-noising," *Sci. Rep.*, vol. 9, no. 1, p. 15181, 2019, doi: 10.1038/s41598-019-51802-9.
[22] C.-M. Lee *et al.*, "Evaluation and improvement of coastal GNSS reflectometry sea level variations from existing GNSS stations in Taiwan," *Adv. Sp. Res.*, vol. 63, no. 3, pp. 1280–1288, 2019, doi: 10.1016/j.asr.2018.10.039.

[23] K. D. Anderson, "Determination of Water Level and Tides Using Interferometric Observations of GPS Signals," *J. Atmos. Ocean. Technol.*, vol. 17, pp. 1118–1127, 2000, doi: 10.1175/1520-0426(2000)017<1118:DOWLAT>2.0.CO;2.
[24] M. Song, X. He, X. Wang, Y. Zhou, and X. Xu, "Study on the Quality Control for Periodogram in the Determination of Water Level Using the GNSS-IR Technique," *Sensors*, vol. 19, no. 20, 2019, doi: 10.3390/s19204524.
[25] C. Roesler and K. M. Larson, "Software tools for GNSS interferometric reflectometry (GNSS-IR)," *GPS Solut.*, vol. 22, no. 80, Jul. 2018, doi: 10.1007/s10291-018-0744-8.
[26] K. M. Larson and F. G. Nievinski, "GPS snow sensing : results from the EarthScope Plate Boundary Observatory," *GPS Solut.*, vol. 17, pp. 41–52, 2013, doi: 10.1007/s10291-012-0259-7.
[27] S. Jin, X. Qian, and H. Kutoglu, "Snow Depth Variations Estimated from GPS-Reflectometry : A Case Study in Alaska from L2P SNR Data," *Remote Sens.*, vol. 8, no. 63, 2016, doi: 10.3390/rs8010063.
[28] N. R. Lomb, "Least-squares Frequency Analysis of Unequally Spaced Data," *Astrophys. Space Sci.*, vol. 39, pp. 447–462, 1976, doi: 10.1007/BF00648343.
[29] J. T. Vanderplas, "Understanding the Lomb–Scargle Periodogram," *Astrophys. J. Suppl. Ser.*, vol. 236, no. 16, 2018.
[30] A. S.-Gómez and C. Watson, "Remote leveling of tide gauges using GNSS reflectometry: case study at Spring Bay, Australia," *GPS Solut.*, vol. 21, no. 2, pp. 451–459, 2017, doi: 10.1007/s10291-016-0537-x.
[31] K. M. Larson, J. S. Löfgren, and R. Haas, "Coastal sea level measurements using a single geodetic GPS receiver," *Adv. Sp. Res.*, vol. 51, no. 8, pp. 1301–1310, 2013, doi: 10.1016/j.asr.2012.04.017.
[32] W. Zhou, L. Liu, L. Huang, Y. Yao, J. Chen, and S. Li, "A New GPS SNR-based Combination Approach for Land Surface Snow Depth Monitoring," *Sci. Rep.*, vol. 9, no. 1, pp. 1–20, 2019, doi: 10.1038/s41598-019-40456-2.

BIOGRAPHIES OF AUTHORS

Agung Syetiawan is a researcher in Geospatial Information Agency of Indonesia. He received Master's Degree in Geodesy and Geomatics Engineering from Institut Teknologi Bandung, Indonesia. His research activities include oceanography, UAV, and GNSS processing.

Dudy Darmawan Wijaya is a researcher and lecturer at Geodesy and Geomatics Study Program, Institut Teknologi Bandung. He received his Ph.D. from Graz University of Technology, Austria. His main research interests are on satellite geodesy and mathematical modeling for GNSS/Geodesy.

Irwan Meilano is a researcher and lecturer at Geodesy and Geomatics Study Program, Institut Teknologi Bandung. He received his Ph.D. from Nagoya University, Japan. His main research interests are on GNSS, geodynamics, and natural hazards